What is Hysteresis?

K. A. Morris*

Hysteresis is a widely occuring phenomenon. It can be found in a wide variety of natural and constructed systems. Generally, a system is said to exhibit hysteresis when a characteristic looping behaviour of the input-output graph is displayed. These loops can be due to a variety of causes. Furthermore, the input-output graphs of periodic inputs at different frequencies are generally identical. Existing definitions of hysteresis are useful in different contexts but fail to fully characterize it. In this paper, a number of different situations exhibiting hysteresis are described and analyzed. The applications described are: an electronic comparator, gene regulatory network, backlash, beam in a magnetic field, a class of smart materials and inelastic springs. The common features of these widely varying situations are identified and summarized in a final section that includes a new definition for hysteresis.

1 Introduction

Hysteresis occurs in many natural and constructed systems.

The relay shown in Figures 1 is a simple example of a system exhibiting hysteretic behaviour. The relay in the Figure is centered at s with an offset of r. When the signal $u > s + r$, the relay is at $+1$. As the input decreases, the output R remains at $+1$ until the lower trigger point $s - r$ is reached. At this point the output switches to -1. When the signal is increasing, the output remains at -1 until $u = s + r$. At this point, the output switches to $+1$. For inputs in the range $s - r < u < s + r$ the output can be $+1$ or -1, depending on past history. Thus, the output may lag the input by $2r$. This lag prevents devices such as thermostats from chattering as the temperature moves just above or below the setpoint. Hysteretic behaviour is also apparent in many other contexts, such as play in mechanical gears and smart materials [1–6]. Hysteresis also occurs naturally in a number of systems such as genetic regulatory systems [2]. All these examples are discussed in more detail later in this paper.

The first mention of hysteresis appeared in an 1885 paper on magnetism [7]. Ewing wrote

> In testing the changes of thermoelectric quality which a stretched wire underwent when successively loaded and unloaded so as to suffer alternate application and removal of tensile stress, I found that during increment and decrement of the load equal values of load were associated with widely different values of thermoelectric quality; the difference being mainly of this character, that the changes of thermoelectric quality lagged behind the changes of stress. This lagging is, however, a *static* phenomenon, for it is sensibly unaffected by the speed at which the load is changed; and again, when any state of load is maintained constant, the thermoelectric quality does not change with lapse of time... Magnetic phenomena present many instances of a similar action- some of which will be described below. Thus, when a magnetised piece of iron is alternately subjected to pull and relation of pull sufficiently often to make the magnetic changes cyclic, these lag behind the changes of stress in much the same way as the changes of thermoelectric quality do. I found it convenient to have a name for this peculiar action, and accordingly called it Hysteresis (from ὕστερέω, to lag behind).

This paragraph highlights two key aspects of hysteresis that are still regarded as characteristic today: "lagging" and rate-independence.

Lagging is still generally regarded as a key component of hysteresis. The online version of the Merriam-Webster dictionary defines hysteresis as

> retardation of an effect when the forces acting upon a body are changed (as if from viscosity or internal friction) ; especially : a lagging in the values of resulting magnetization in a magnetic material (as iron) due to a changing magnetizing force. [8]

In the simple relay shown in Figure 1, changes in the output lag changes in input. However, the output of a linear delay system such as $y(t) = u(t-1)$ also lags the input. Such systems would not be described as hysteretic.

The second property mentioned by Ewing, rate independence, means that an input/output plot only depends on the values of the input, but not the speed at which the input is changed. In a rate-independent system such as those shown in Figures 1 and 2 the input/output plot with input $u(t) = M\sin(t)$ is identical to that with $u(t) = M\sin(10t)$. More formally, let a differentiable function $\varphi : \mathbb{R}_+ \to \mathbb{R}_+$ be a *time transformation* if $\varphi(t)$ is increasing and satisfies

*Dept. of Applied Mathematics, University of Waterloo, Waterloo, Ontario, Canada, (kmorris@uwaterloo.ca) .

$\varphi(0) = 0$ and $\lim_{t\to\infty} \varphi(t) = \infty$. For any interval $I \subset \mathbb{R}_+$, let $Map(I)$ indicate the set of real-valued functions defined on I.

Definition 1. *[9] An operator $\Gamma : \mathbb{U} \subset Map(I) \to Map(I)$ is* rate independent *if for all time transformations φ, and all inputs $v \in \mathbb{U}$,*

$$(\Gamma v) \circ \varphi = \Gamma(v \circ \varphi).$$

In [10, pg. 13] hysteresis is defined as rate independence combined with a *memory effect*, or dependence of previous values of the input.

True rate independence implies that the system is able to transition arbitrarily quickly. For physical systems this is an idealization. For instance, in the magnetic materials discussed in the above quote, changes in magnetization are controlled by a characteristic time constant. Furthermore, thermal fluctuations means that magnetization can change even when the input doesn't change. Thus, rate independence in magnetic materials is an approximation valid when thermal effects are low and the input does not change extremely fast. Similarly, it is not possible to vary the temperature of a shape memory alloy arbitrarily quickly, so from a practical point of view, the temperature-strain curves in these materials typically display rate independence. Rate independence/dependence in the context of various examples is discussed later in this paper.

Definition 2. *[1, 10]. An operator $\Gamma : \mathbb{U} \subset Map(I) \to Map(I)$ that is both causal and rate-independent is said to be a hysteresis operator.*

This definition has been quite useful in analysis of systems involving hysteresis - see for example, [12–15]. However, there are a couple of difficulties with this approach. First, the definition is so general that it can include systems which would not typically be regarded as hysteretic. A trivial example is $y = u$; another is $y(t) = u(t-1)$. Furthermore, as mentioned above, many systems regarded as hysteretic have behaviour that is rate-independent at low input rates but rate-dependent at high input rates.

Another typical characteristic of hysteretic systems is looping behaviour, illustrated in Figures 1 and 2. One standard text [1] writes: *When speaking of hysteresis, one usually refers to a relation between 2 scalar time-dependent quantities that cannot be expressed in terms of a single value function, but takes the form of loops.* However, the loop shown in Figure 3 is produced by a system that would not be described as hysteretic. This linear system is clearly not rate-independent and the curves produced by a periodic input will converge to a line as the frequency approaches zero. In fact, any loop in the input-output curve of a linear system with a periodic input degenerates to a single curve as the input frequency decreases. In [16], it is suggested that systems for which the input-output map has non-trivial closed curves that persist for a periodic input as the frequency of the input signal approaches zero be regarded as hysteretic. This is useful as a test since it excludes systems (such as the linear system in Figure 3) where the looping is a purely rate-dependent phenomenon. However, in magnetic materials, magnetism can approach the single-valued anhysteretic curve as the rate of change of the applied field approaches zero [17]. Since the response of a system to an input is affected by the history of the current input (see again the simple relay in Figure 1), hysteretic systems are often described as having *memory*. The state x in the familiar dynamical system description $\dot{x}(t) = f(x,t)$ encodes the memory of a system. Knowledge of the current state, and the inputs is sufficient to determine the output. Consider a simple integrator:

$$\begin{aligned} \dot{x}(t) &= u(t) \\ y(t) &= x(t). \end{aligned}$$

The output y is the integral of the input u and the state x stores the memory of the system, the current state of the integrator. This linear system would not be described as hysteretic.

In this paper a number of common examples of systems that are said to be hysteretic are examined in detail: an electronic trigger, a biological switch, smart materials, mechanical play and inelastic springs. A model for a magneto-elastic beam is also analysed and shown to display hysteretic behaviour. The common features of these systems are analysed and used to formulate a definition of hysteresis. This paper is not intended to be a review of the extensive literature on hysteretic systems. Some previous works that do provide reviews are [1, 4, 10, 18].

2 Schmitt Trigger

A comparator or switch changes its output from some level y_- to y_+ when the input increases above a reference level. Conversely, the output is dropped from y_+ to y_- as the input drops below the reference level. A familiar example is a household thermostat where the furnace is turned on when the room temperature falls below the set-point, and turned off when the temperature rises above the setpoint. The problem with a simple switch is that there is a tendency to oscillate about the setpoint as the input falls slightly above or below the setpoint. Such oscillations can be caused by noise alone. For this reason, more complicated comparators with a response similar to that of the simple relay shown in Figure 1 are used.

A common way to implement such a device is a circuit known as a Schmitt trigger [19]. The idea for this device arose as part of Otto Schmitt's doctoral work in the 1930's on developing an electronic device to mimic the generation and propagation of action potentials along nerve fibres in squid. Schmitt continued his work in biophysics and is credited with developing the word *biomimetics* towards the end of his career. [20].

A Schmitt trigger is used today in many applications, such as thermostats and reduction of chatter in circuits [3].

Experimental response of a Schmitt trigger is shown in Figure 4. It is apparent that the response of a Schmitt trigger is similar to that of the simple relay shown in Figure 1.

Although Schmitt's original realization [19] used vacuum tubes, current implementations use electronics, such as the operational amplifier (op amp) shown in Figures 5. In theory, an op amp multiples (amplifies) the input voltage v by a fixed amount, say A, to produce an output voltage Av. In practice, this amplification only occurs in a certain range of voltage and op amps saturate beyond a certain point. The maximum and minimum voltages are contained within fixed limits. Elementary descriptions of the behaviour of a Schmitt trigger, for example, that in [21] use the basic circuit diagram Figure 5a and rely on the fact that the op amp saturates beyond a certain point. The analysis is separate for each operating region and depends on whether the input is increasing or decreasing.

A better understanding of the trigger's behaviour can be obtained by using a more accurate model for the op amp that includes its capacitance, as shown in Figure 5b. The stability analysis on the differential equation that describes this circuit predicts the behaviour of the Schmitt trigger [3]. Consider the equivalent circuit shown in Figure 5c where the active element f describes a finite-gain op-amp. Let $E_- > 0$ and $E_+ > 0$ denote the lower and upper saturation voltages respectively, $A \gg 1$ the op amp gain, and define

$$f(v) = \begin{cases} -E_- & v \le -\frac{E_-}{A} \\ Av & -\frac{E_-}{A} < v < \frac{E_+}{A} \\ E_+ & v \ge \frac{E_+}{A} \end{cases} \tag{1}$$

so that $v_o = f(v)$. For simplicity in this analysis we will assume the upper and lower saturation voltages are symmetric: $E_- = E_+ = E$.

The input in this case is the input voltage v_i, while the output is the op amp output voltage v_o. Defining

$$g(v_i, v) = G_i(v_i - v) + G_f(v_o - v) \tag{2}$$

where $v_o = f(v)$ and $G_i = \frac{1}{R_i}$, $G_f = \frac{1}{R_f}$, application of Kirchoff's Current Law to the circuit in Figure 5c yields the differential equation for the capacitor voltage v,

$$C_p \frac{dv}{dt} = g(v_i, v). \tag{3}$$

The capacitance C_p is very small, about $10^{-11}F$; see for example, [21, chap. 11], although this value can be even smaller in some op amp configurations. Typical values of $R_i = 10k\Omega$, $R_f = 20k\Omega$, $A = 10^5$ and $C_p = 15\ pF$ yield a settling time of $40\mu s$. Because of these fast transients, in practice only the equilibrium values of the variables are observed. This is illustrated by the graphs in Figure 6. Note the similarity to the graph of a simple relay. Thus a quasi-static analysis of the relationship of the output voltage v_o to the capacitor voltage v, with the input voltage v_i regarded as fixed is appropriate.

The equilibrium values of v for any specific input voltage v_i are the zeros of $g(v_i, v)$. The function $v \to g(v_i, v)$ with $v_i = 1$ and the above parameter values is plotted in Figure 7. Note that since A is very large, the middle portion of the graph, where g is increasing, appears vertical in comparison to the other sections. The function g reaches a maximum value of

$$I_{max} = G_i v_i + \frac{E}{A}\big((A-1)G_f - G_i\big)$$

at $v = \frac{E}{A}$ and a minimum value of

$$I_{min} = G_i v_i - \frac{E}{A}\big((A-1)G_f - G_i\big)$$

at $-\frac{E}{A}$. If $I_{min} < 0$ and $I_{max} > 0$ (as shown in Figure 7) then $g(v_i, \cdot)$ has 3 real roots and there are 3 equilibrium points. Defining $\bar{v} = \frac{G_f}{G_i}E$, $\alpha = \frac{G_i}{G_f + G_i}$, these equilibrium points are

$$\alpha(v_i - \bar{v}), \qquad \frac{G_i v_i}{G_f + G_i - G_f A}, \qquad \alpha(v_i + \bar{v}).$$

If either $I_{min} = 0$ or $I_{max} = 0$ then there are 2 equilibrium points. If the input voltage v_i is such that $I_{min} > 0$ or $I_{max} < 0$ then $g(v_i, \cdot)$ has only one real zero and so there is only 1 equilibrium point.

The stability of the equilibria can be analysed by examining $\frac{\partial g}{\partial v}$. For $|v| \ge \frac{E}{A}$,

$$\frac{\partial g}{\partial v} = -G_f - G_i < 0$$

and the corresponding equilibrium is stable. On the other hand for $|v| < \frac{E}{A}$,

$$\frac{\partial g}{\partial v} = (A-1)G_f - G_i > 0$$

since $A >> 1$. Thus, equilibria that occur in the linear region of operation of the op amp are unstable, and are not observed due to noise in the system. Equilibria in the saturation region of the op amp are stable.

To understand further the behaviour of the system as the input voltage varies, define

$$\mathcal{E}_{v_i}(v) = \begin{cases} \frac{1}{2}(v + \alpha\bar{v})^2 - \alpha v_i v & v \le -\frac{E}{A}, \\ \frac{1}{2}(\alpha\bar{v} - \frac{E}{A})(\alpha\bar{v} - \frac{v^2}{\frac{E}{A}}) - \alpha v_i v & |v| < \frac{E}{A}, \\ \frac{1}{2}(v - \alpha\bar{v})^2 - \alpha v_i v & v \ge \frac{E}{A}. \end{cases} \tag{4}$$

This function has minima at the stable equilibrium points v_e of the system. If it is shifted by a constant for each input voltage v_i so that $\mathcal{E}_{v_i}(v_e) = 0$, it is a Lyapunov function for the system. (See [22, e.g.] for a definition and discussion of Lyapunov functions.) This function is plotted for varying values of v_i in Figures 9. Suppose the system starts with a low input voltage v_i so that there are 3 equilibrium points and the voltage $v < \frac{-E}{A}$ is at the smallest equilibrium point: $v = \alpha(v_i - \bar{v})$.The op amp is in negative saturation, with $v_o = -E$, as shown on Figure 8 for the case $E = 4$. For low values of v_i, the Figures 9a and 9b are appropriate. As v_i increases, the smallest zero of g increases, and v increases slowly. The output voltage remains at $-E = -4$. The 2 lower zeros move closer together until there are only 2 zeros of g. This occurs when the input voltage is equal to

$$v_{crit} = \bar{v} - \frac{E}{\alpha A}.$$

Since $A >> 1$, $v_{crit} \approx \bar{v}$. (The parameter values used here lead to $v_{crit} \approx 2$.) At this point the only stable equilibrium point is the largest zero of g and the output value increases rapidly to the new equilibrium point. This is shown in Figure 9d. The op amp will be in positive saturation with $v_o = E$, the upper value on Figure 8. Since in practice the input voltage changes much slower than the settling time of the system, this change appears instantaneous. For large values of the input, there is only one stable equilibrium point and v increases linearly with further increases in the input. Since the op amp is saturated, there is no change in v_o. A similar process happens when v_i decreases, but now v is maintained at the upper equilibrium point until this point coalesces with the middle unstable equilibrium point; that is at $v_i = -\bar{v}_i$. This process is illustrated by Figures 9e-h. When v moves to the lower equilibrium point, the output v becomes $-E$, the lower value on Figure 8.

This analysis of the differential equation (3) modelling the Schmitt trigger shows that the fact that two different output voltages are possible for a given input voltage is due to the presence of two stable equilibrium points of the capacitor voltage. The transition between different equilibrium values appears to be immediate due to the fast transients in this system. The combination of these properties lead to the relay-like behaviour that makes this device useful.

3 Cell Signaling

There exist biological "switches", which analogously, to an electronic switch such as the Schmitt trigger, have a steady-state value that is changed by an external signal. Moreover, this new value is maintained even when the signal is removed. Thus, the switch can be said to have a memory of the previous input value.

One of the simplest examples of a such a switch consists of a pair of two genes which repress each other by expressing protein transcription factors. These switches occur in genetic regulatory systems. A general model for such a network is

$$\dot{x}_1(t) = F(x_2) - \mu_1 x_1,$$
$$\dot{x}_2(t) = G(x_1) - \mu_2 x_2$$

where x_1, x_2 indicate two *repressor proteins*, F and G are functions to be determined and μ_1, μ_2 are positive constants. In [23] it is shown that F and G must have multiple equilibrium points in order for the system to display switching behaviour. A common family of models for a two-repressor system that does lead to a system that has multiple equilibrium points and thus displays "memory" is

$$\dot{x}_1(t) = \frac{\alpha_1}{1 + x_2^{\beta_1}} - x_1, \tag{5}$$
$$\dot{x}_2(t) = \frac{\alpha_2}{1 + x_1^{\beta_2}} - x_2 \tag{6}$$

where α_i, β_i are positive constants. Equilibrium points are solutions to the system of equations

$$x_1 = \frac{\alpha_1}{1 + x_2^{\beta_1}},$$
$$x_2 = \frac{\alpha_2}{1 + x_1^{\beta_2}}.$$

Substituting the first equation into the second, and regarding the repressor protein x_2 as the output y of this system, equilibrium values of y correspond to fixed points of

$$F(y) = \frac{\alpha_2 (1 + y^{\beta_1})^{\beta_2}}{(1 + y^{\beta_1})^{\beta_2} + \alpha_1^{\beta_2}}.$$

For certain values of the parameters, the equation $y = F(y)$ has 3 roots and hence the system has three equilibrium points. In [2] the above model is used to describe a genetic toggle switch. Parameter values of $\alpha_1 = 156.25$, $\beta_1 = 2.5$, $\alpha_2 = 15.6$, $\beta_2 = 1$ are used. These values yield three equilibrium points. Analysis of the linearization of (5,6) about each equilibrium point shows directly that two of these equilibrium points are stable while the third (the middle value of x_2 or y) is unstable.

If the concentration of one of the repressors is perturbed from one stable equilibrium point, the system will return to this point if the perturbation is not large. A larger perturbation could move the system into a region around the other stable equilibrium point. The system will then settle at this new equilibrium point.

Equations (5,6) can be rewritten as the feedback system

$$\dot{x}_1(t) = \frac{\alpha_1}{1 + u^{\beta_1}} - x_1,$$
$$\dot{x}_2(t) = \frac{\alpha_2}{1 + x_1^{\beta_2}} - x_2,$$
$$y = x_2,$$

with the connection $u = y$. The first two equations are a monotone system [24,25]. In [25] the stable equilibria of this system are found using [25, Thm. 3]. This approach can be useful for high-dimensional systems. It is argued in [26] that bistability, along with hysteretic behaviour, is often found in biological systems with feedback-connected monotone systems.

In this system, the active form of the protein x_1 is repressed by isopropyl-β-*D*-thiogalactopyranoside (IPTG), and this leads to an increase in x_2 (y). Letting u indicate the level of IPTG, the model is modified [2] so that instead of x_1 in (6) is replaced by

$$\frac{x_1}{(1+u/K)^\eta} \tag{7}$$

where K, η are positive constants. (Values of $K = 2.9618 \times 10^{-5}$ and $\eta = 2.0015$ are used in [2].) Figure 10 shows the equilibrium values of $y = x_2$ against u. For the range $-10^{-6} < u < 4 \times 10^{-5}$ there are 3 equilibrium values. Analysis shows that the middle one is unstable, while the others are stable.

In practice, the level of IPTG is changed over a number of hours. Figure 11 shows a plot of y against u as u increases. Little change is seen in y until u reaches a critical value of $40\mu M$. At that point, the level of y jumps sharply to the second equilibrium value, as shown in Figure 11. Since the dynamics of the system are very fast compared to the rate at which IPTG can be changed, this transition appears instantaneous. The upper value of y is maintained when the control u is subsequently decreased. The predictions of this model are shown in [2] to closely match experimental data. However, due to natural fluctuations, as well as stochastic effects in the system, the experimental transition is less abrupt than shown here.

The opposite switch, that of lowering y, in theory can be accomplished by lowering u to the point that the upper equilibrium point disappears. However, as illustrated in Figure 10 the drop to a single equilibrium value occurs for negative values of u. Since u, the amount of IPTG, must be non-negative this is not possible in practice. The "off" switch, or lowering of y, is accomplished in this system by temperature modulation. The activity of the protein y is temperature sensitive. An increase in temperature shifts y to an inactive state. To model this, (5,6) needs to be modified to include a dependence on temperature. A model for this not given in [2]. However, experimental data is provided that shows that y drops as temperature is increased and that this lower level is maintained when the temperature is subsequently lowered.

Thus, bistability is the mechanism behind the memory, or hysteresis, in this 2-repressor genetic switch. Bistability is responsible for switching and hysteretic behaviour in a number of other biochemical systems; see for instance, examples in [23, 26, 27].

4 Beam in a Magnetic Field

Consider a flexible beam or other structure operating within a magnetic field. Examples include transformers, disc drives and magnetically levitated vehicles. If the structure is composed of a ferromagnetic material, the presence of the magnetic field affects its deformation. Although the structure itself does not become magnetized to a significant extent, the magnetic field exerts a force on the structure. Consider the situation, shown in Figure 12, where there are two different magnetic sources. A nonlinear partial differential equation for the beam deflection $w(t)$ in the configuration shown in Figure 12 was developed in [5].

Since the first mode is dominant, it is relevant to examine only the first mode. This leads to an ordinary differential equation for the coefficient $a(t)$ of the first mode:

$$\ddot{a}(t) + \delta\dot{a}(t) - \alpha a(t) + \beta a(t)^3 + \eta a(t)^5 = f(t)$$

where $f(t)$ is a forcing term. The effective stiffness of the beam, α, includes both elastic and magnetic terms. The coefficients β and η depend on the local magnetic field. In general, the highest order term $\eta a(t)^5$ does not affect the qualitative behaviour and is neglected in the analysis [5]. Converting to dimensionless variables using the characteristic length $\sqrt{\frac{\alpha}{\beta}}$ and time $\frac{1}{\sqrt{2\alpha}}$, yields the normalized equation

$$\ddot{A}(\tau) + d\dot{A}(\tau) - \frac{1}{2}A(\tau)\big(1 - A(\tau)^2\big) = u(\tau) \tag{8}$$

where $d = \frac{\delta}{\sqrt{2\alpha}}$ and $u(\tau)$ is the forcing term in the new variables. Considering only the first mode of a complex system may seem to be a gross over-simplification. However, experimental results support the qualitative analysis [5, 28]. More generally, this equation describes the motion of a unit mass subject to the non-convex potential

$$V(x) = \frac{x^4}{8} - \frac{x^2}{4}$$

as well as viscous damping and an external force u.

Equation (8) is a type of Duffing oscillator [29, pg. 82-91, e.g.]. It is often studied as a relatively simple illustration of a chaotic system [5, 28, 30, 31]. However, we are interested here in how the stability of the system changes as the magnetic field u varies.

Writing the equation (8) in standard first-order form with $x = [A,\ \dot{A}]$ yields

$$\begin{aligned} \dot{x}_1(\tau) &= x_2(\tau) \\ \dot{x}_2(\tau) &= -dx_2(\tau) + \tfrac{1}{2}x_1(\tau)\big(1 - x_1(\tau)^2\big) + u(\tau). \end{aligned} \tag{9}$$

For constant inputs $u(\tau) = M$, the system has equilibrium points given by $(x_e, 0)$ where x_e solves

$$\frac{1}{2}x\big(1 - x^2\big) + M = 0.$$

The unforced system, $M = 0$, has 3 equilibrium points, $(1,0)$ and $(-1,0)$ and $(0,0)$. Analysis of the Jacobian shows that $(1,0)$ and $(-1,0)$ are stable while $(0,0)$ is unstable. For $|M| < \frac{1}{3\sqrt{3}} \approx 0.2$, there are 3 real roots of this equation, and hence 3 equilibria. The middle equilibrium point is unstable while the outer two are stable. However, for larger inputs $|M| > \frac{1}{3\sqrt{3}}$ these reduce to one equilibrium point. This is illustrated in Figure 13 .

Suppose the system starts with a small value of u, so the system is at the lowest equilibrium. As u is increased, this equilibrium value increases slowly. When u increases above 0.2, this equilibrium disappears and the system moves to the new equilibrium. This change is almost instantaneous compared to the rate of change of u. When u is decreased, the system remains at this larger equilibrium point until u is decreased below -0.2, at which point this equilibrium point disappears and the system moves rapidly to the new equilibrium. For $-0.2 < u < 0.2$ there are several equilibria and the state of the system can be at either of the stable equilibrium points.

For an input with magnitude in $[0, .25]$, the characteristic frequency of the system linearized around a stable equilibrium point is between 1 and 1.27. Thus, for input frequencies $\omega << 1$ we expect the system to display rate independent behaviour. This is illustrated in Figure 14a, which shows input/output diagrams of the system under periodic inputs $u(t) = 0.25\sin(\omega\tau)$ where $\omega < 10^{-4}$. In Figure 14b the response of the system to periodic inputs with larger frequencies is shown. Although the same looping behaviour is observed as the system moves between different equilibrium points, the input-output diagrams are rate-dependent. This is expected, since at frequencies closer to 1, the rate of change of input becomes comparable to the system dynamics.

The curves shown in Figures 14 are very similar in appearance to those of the hysteretic systems examined in previous sections. The looping behaviour characteristic of hysteretic systems is apparent. As for the other examples, the current state, or history, of the system affects the output. At low input rates, the system moves to a new equilibrium almost instantaneously compared to the rate of change of the input. Thus, at slow rates, the curves appear rate-independent. However, at faster rates, approaching the fundamental frequency of the system, rate-dependence becomes apparent.

5 Backlash

One of the simplest examples of a system exhibiting hysteresis is backlash, sometimes called play [1, 10]. It occurs in many mechanical systems. For instance, it describes slippage in gears that do not perfectly mesh such as those shown in Figure 15.

A graphical description of the behaviour of a play operator is shown in Figure 16. The rod with position $w(t)$ is moved by a cart of width $2r$ with centre position $u(t)$. As long as the rod remains within the interior of the cart, the rod does not move. Once one end of the cart reaches $w(t) = u(t)$, the rod will move with the cart. For any piecewise monotone input function $u(t)$ let $0 = t_0 < t_1 < t_2 < \ldots < t_N = t_E$ be the partition of $[0, t_E]$ such that the function u is monotone on each of the subintervals $[t_i, t_{i+1}]$. On an interval where $u(t)$ is increasing ($u(\tau_1) > u(\tau_2)$ if $\tau_1 > \tau_2$), the behaviour of the play operator can be written formally as

$$\begin{aligned} w(t) &= w(t_i), & w(t) > u(t) - r \\ &= u(t) - r, & w(t) \le u(t) - r. \end{aligned} \tag{10}$$

If $u(t)$ is decreasing on an interval,

$$\begin{aligned} w(t) &= w(t_i), & w(t) < u(t) + r \\ &= u(t) + r, & w(t) \ge u(t) + r. \end{aligned} \tag{11}$$

Alternatively, the play operator can be described by [1, pg. 24-25]

$$\begin{aligned} w(0) &= f_r(u(0), 0), \\ w(t) &= f_r(u(t), w(t_i)), \ t_i \le t \le t_{i+1}, \ 0 \le i \le N-1, \end{aligned} \tag{12}$$

where

$$f_r(u, w) = \max\{u - r, \min\{u + r, w\}\}.$$

This model is quite different from those discussed in the previous sections in a number of respects. First, the models discussed earlier displayed rate-independent behaviour for input rates significantly faster than the system dynamics. However, this model has no dynamics and is actually rate-independent. Since it is also causal, it defines a hysteresis operator.

Furthermore, since this model has no dynamics, any solution w is an equilibrium solution. In other words, any point w with $|u - w| \le r$ is an equilibrium point. Thus, there is a continuum of equilibrium points. The models described above have a discrete number of equilibrium points. Since the model is static, any equilibrium point can be regarded as stable.

By introducing an internal variable $v(t)$ for the cart position, the operator can be approximately described by a differential equation. Let $a > 0$ be a constant, large compared to the rate of change of the input $u(t)$ and define

$$\begin{aligned} \dot{v}(t) &= a\big(u(t) - v(t)\big) \\ \dot{w}(t) &= g\big(u(t), v(t), w(t)\big) \end{aligned} \tag{13}$$

where

$$g(u, v, w) = \begin{cases} a(u - v), & u - v > 0 \text{ and } w - v \le -r, \\ a(u - v), & u - v < 0 \text{ and } w - v \ge r, \\ 0, & \text{otherwise.} \end{cases}$$

This model can be thought of incorporating some dynamics for the movement of the cart so that it does not instantaneously move to a new position v in response to the control u. The state variable v is in equilibrium whenever $v = u$. The other state variable, w, is also the output. It is in equilibrium whenever $v = u$ or $|v - w| \leq r$. The equilibrium value of w depends on v. Provided that a is chosen very large compared to how quickly u is varied, the system will only be observed in equilibrium.

Numerical integration of this equation for several periodic inputs of varying frequency are shown in Figure 17. The output is identical to that of the static model. Thus, for the given range of frequencies, this dynamical system displays the rate-independent looping behaviour characteristic of hysteretic systems. Although the differential equation (13) provides insight into the nature of the system, and may be useful for calculations requiring a differential equation model, it is slower to solve than the static model (12).

6 Smart materials

Smart materials, such as piezo-electrics, shape memory alloys and magnetostrictives, are becoming widely used in a number of industrial and medical applications. A more accurate term for these materials would perhaps be *transductive* actuators, since they all transform one form of energy into another. Piezo-electric materials transform electrical energy into mechanical energy. Shape memory alloys transform thermal energy into mechanical and can replace mechanical motors in some applications. Magnetostrictives transform magnetic into mechanical energy, in response to an applied magnetic field. This transductive quality means that smart-material-based actuators are generally lighter and more reliable than traditional actuators with comparable power.

Although these materials involve quite different processes, they are all display typical hysteretic behaviour. The reason for this is the existence of a non-convex energy potential. Consider, as an example, a magnetostrictive material such as Terfenol-D. The material is considered to be composed of magnetic dipoles. The following simplified explanation is quite brief; for details see [6].

Letting M indicate the magnetization for the dipole, ε total strain, M_R, η, γ_1 and Y physical constants, and defining

$$f(M) = \begin{cases} \frac{\mu_0\eta}{2}(M+M_R)^2, & M \leq -M_I, \\ \frac{\mu_0\eta}{2}(M-M_R)^2, & M \geq M_I, \\ \frac{\mu_0\eta}{2}(M_R-M_I)(M_R-\frac{M^2}{M_I}), & |M| < M_I, \end{cases},$$

the Helmholtz free energy of each dipole can be described by [6]

$$\psi(M,\varepsilon) = \frac{1}{2}Y\varepsilon^2 - Y\gamma_1\varepsilon M^2 + f(M). \tag{14}$$

In the absence of strain ε, ψ has local minima at $\pm M_R$. The parameter M_I is the inflection point where the second derivative of ψ changes sign.

Letting H_o indicate the magnetic field, the Gibbs energy for each dipole is

$$G(H_o,M,\sigma,\varepsilon) = \psi(M,\varepsilon) - \mu_0 H_0 M. \tag{15}$$

Figure 19 shows the Gibbs energy versus magnetization at different values of the magnetic field. The equilibrium magnetization M of each dipole occurs at a minimum of the Gibb's energy and so the magnetization M for the dipole can be obtained using the condition

$$\left(\frac{\partial G(H_o,M,\sigma,\varepsilon)}{\partial M}\right)_{H_o,\sigma,\varepsilon} = 0. \tag{16}$$

Thermodynamic equilibrium is obtained faster than the rate at which the magnetic field is changed. The system is observed only at equilibrium. As seen in Figure 19(a), if $H_o = 0$, two minima of G exist:

$$M_-^* = \frac{H_o}{\eta} - M_R, \tag{17}$$

$$M_+^* = \frac{H_o}{\eta} + M_R. \tag{18}$$

For a small positive H_o as shown in Figure 19(b), still two minima exist, but if H_o is further increased, so that $H_o > H_c$ where

$$H_c = \eta(M_R - M_I),$$

the left-hand minimum M_-^* disappears as shown in Figure 19(c). Similarly, for $H_o < -H_c$, the right-hand minimum does not exist. The critical magnetic field H_c is called the coercive field.

Suppose the system is initially at a magnetization level M_-^* with $H_o = 0$. As H_o is increased, the magnetization is given by (17) until $H = H_c$. At this point the magnetization is still given by (17), but as H is increased further, eventually this equilibrium point disappears and there is only the equilibrium point M_+^* (18). At this time, dipole magnetization moves rapidly to the right-hand equilibrium, M_+^*. This transition is shown with an arrow in Figure 19(c). If the field H is subsequently decreased the magnetization is given by the right-hand equilibrium M_+^* until $H < -H_c$. At this field level, the right-hand minimum M_+^* disappears and the magnetization moves rapidly to the left-hand equilibrium M_-^*.

The above model can be improved in a number of respects; for instance by modifying the Gibb's energy to include a more accurate description of the effect of magnetostriction [33, 34].

The macroscopic behaviour of a material is more difficult to describe. Suppose we consider the material to be a sum of dipoles. The parameter M_R, known as the remanence magnetization, is the same for all dipoles. However, the inflection point M_I varies. Also, since the local field H_o at each

dipole is affected by imperfections and non-homogeneties, it is not equal to the applied magnetic field H. Assume that the interaction field $H_I = H - H_o$ between the external and local magnetic fields is constant over time for each dipole. The parameters H_I and M_I (as well as the history of H) determine the magnetization at each dipole. However, it is convenient to use H_c instead of M_I so that the 2 parameters are H_I and H_c.

The Gibb's energy is minimized for each dipole. The memory of the system is the state of each individual dipole, that is, whether it is in the left or right equilibrium. Let $M^*(H_I, H_c; H)$ indicate the magnetization, M^*_+ or M^*_-, associated with dipoles with interaction field H_I, coercive field H_c and input history H. The variable H indicates that magnetization depends on the applied magnetic field. Assuming a distribution of ν_1 for the interaction field H_I and ν_2 for the coercive field H_c yields an overall magnetization

$$M = \int_0^\infty \int_{-\infty}^\infty M^*(H_I, H_c; H)\nu_1(H_I)\nu_2(H_c)dH_I dH_c. \quad (19)$$

Since different dipoles have different transition points, this model leads to a smooth transition in the value of M as the applied field H is changed. This aspect of the model is supported by experimental results. Unlike a simple relay (Figure 1) or Schmitt trigger (Figure 4), the input/output diagrams of smart materials (see Figures 2 and 18) do not possess a sharp transition. As for magnetostrictives, the hysteretic behaviour in shape memory alloys and piezo-electrics can be explained by the fact that the equilibrium state minimizes a non-convex energy potential, yielding a model similar in structure to (19).

The above model is a special type of Preisach model [1], a popular class of models for smart materials. In a Preisach model, the model is considered to be composed of an infinite set of simple relays such as that in Figure 1. The centre s and width r of the relays varies, and a weight function $\mu(r,s)$ incorporates the relative weighting of each relay $R(r,s;H)$. This leads to a model of the form

$$M = \int_0^\infty \int_{-\infty}^\infty R(r,s;H)\mu(r,s)dsdr \quad (20)$$

where $R = \pm 1$ is the output of a simple relay (Figure 1) centred at s with width r and history H. By connecting r with H_c and s with H_I, there are clear similarities between (19) and (20). A comparision in the context of Terfonel-D can be found in [32].

In the model (20) (or (19)) relays (or dipoles) in the $+1$ state are separated from the relays at -1 by a boundary curve $\psi(t,r)$ in the $r-s$ plane. The operator (20) can be rewritten

$$M = 2\int_0^\infty \int_0^{\psi(t,r)} \mu(r,s)dsdr + w_0 \quad (21)$$

where

$$w_0 = \int_0^\infty \int_{-\infty}^0 \mu(r,s)dsdr - \int_0^\infty \int_0^\infty \mu(r,s)dsdr.$$

It has been shown that the Preisch model (21) with the boundary $\psi(t,r)$ as the state is a dynamical system [35]. Although there is no dynamics in this model, the state transition operator associated with the state $\psi(t,r)$ satisfies the required axioms including causality and the semigroup property. However, unlike typical dynamical systems, this system is always in equilibrium. Time-dependence only appears implicitly in the input variable $H(t)$. For all constant inputs H, any solution is an equilibrium solution.

Alternatively, the boundary function can be written $\psi(t,r) = \mathcal{F}_r[H](t)$ where $\mathcal{F}$ is the play operator with width r [1]. Thus, the system can be written as an infinite-dimensional system where the state is the state of the family of play operators obtained as width r varies.

Since the models (19) and (21) are static, it is straightforward to show that they are rate-independent. Like the play operator, these models are hysteresis operators. The fact that there are no dynamics and that all solutions are equilibrium solutions reflects the assumption that magnetization is always at its equilibrium value. Since thermodynamic equilibrium is reached much faster than the field can be varied, this assumption is accurate under certain conditions. Efficient methods using the static operator (19) or (21) are used in simulations.

Rate dependence can often be observed in smart materials. For instance, in magnetic materials, thermal activation can lead to a dipole "jumping" from one equilibrium point to another. Unless thermal effects are small and the corresponding time constant small compared to the input frequency, this needs to be considered. This is the basis of the homogenized energy model [6] and also the model in [17]. See also [36] for a similar approach to modelling of shape memory alloys. Equation (19) is the limiting case of this model where these effects are neglected. Furthermore, other effects such as heating dynamics and mechanical dynamics interact with the thermodynamics described above. For example, heating of shape memory alloys is generally accomplished through applying a current. Heating of the material leads to phase transition and an associated change in strain. The rate at which the material is heated affects the resulting phase change. In magnetostrictive materials, a quickly varying current causes a moving magnetic field and can lead to an induction of the current source into a surrounding conductor around the magnetostrictive solid. This affects the magnetic field seen by the material and leads to observation of rate dependence. Including a model for the dynamics of this process, along with a static model for the hysteresis addresses this effect; see for example, [37].

Another approach to modelling the behaviour of smart materials is to derive the dynamical equations using thermodynamic principles. One example of this is the Falk partial differential equation model for shape memory alloys [1].

There is little experimental verification available for this model. However, it does agree qualitatively with experimental data [38], producing plots that display loops and rate independence for standard inputs with low frequencies.

7 Inelastic springs

In the classic Hooke's law, the force of a deformed spring is linearly proportional to the displacement: $F = -kx$. However, many materials do not display this linear elastic behaviour. The Bouc-Wen model [39] has been used to describe inelastic behaviour [40] in a number of applications, including caissons [41], bridge pilings [42] and magnetorheological dampers [43]. A version of the Bouc-Wen model, the Dahl model, has been used to describe friction in several contexts [44, 45].

The Bouc-Wen model, with input x and output Φ, is

$$\begin{aligned} \dot{z}(t) &= D^{-1}\left(A\dot{x}(t) - \beta|\dot{x}(t)||z|^{n-1}z - \gamma\dot{x}(t)|z(t)|^n\right), \\ \Phi(x,z) &= \alpha k x(t) + (1-\alpha)Dkz(t), \\ z(0) &= z_0. \end{aligned} \tag{22}$$

The variable z is an internal state that represents the "memory" of the spring. The real parameters $D > 0$, A, γ, β, $k > 0$ and $0 \le \alpha < 1$ and $n \ge 1$ are chosen to fit experimental data. If $A > 0$ and $-\beta < \gamma \le \beta$ then the output Φ is bounded for bounded x [39]. As mentioned above, the Bouc-Wen model is frequently used as a model for a nonlinear spring or friction and is thus often found combined with a second-order system that represents the structure or system involved; for instance,

$$m\ddot{x}(t) + d\dot{x}(t) + \Phi(x,z) = f(t)$$

where m indicates mass, d damping, and $f(t)$ represents any external forces.

To determine equilibrium points for the Bouc-Wen model, consider a constant input ($\dot{x}(t) = 0$). Then $\dot{z}(t) = 0$ for any value of z and there is a continuum of equilibrium points. This is similar to the situation for the play, Preisach and homogenized energy models discussed in sections 5 and 6.

The input-output behaviour of a Bouc-Wen model is illustrated in Figures 20. The looping behaviour typical of hysteretic systems is apparent in Figure 20b. The system also appears to be rate-independent, at least at the frequencies used in the simulations.

To determine whether the differential equations (22) describe a rate-independent system, we use Definition 1. Let τ and t be two time-scales related by a time transformation $\tau = \varphi(t)$. Recall that for any time transformation, $\dot{\varphi}(t) > 0$. Let the state and output of (22) with input $x(t)$ be $z(t)$ and $\Phi(t)$ respectively and similarly, let the state and output with input $x(\varphi(t))$ be $z_\varphi(t)$ and $\Phi_\varphi(t)$. We need to show that $\Phi_\varphi(t) = \Phi(\varphi(t))$. For simplicity, we let $D = 1$ in (22).

$$\begin{aligned} \dot{z}_\varphi(t) &= A\tfrac{dx}{d\tau}\dot{\varphi}(t) - \beta|\tfrac{dx}{d\tau}|\dot{\varphi}(t)|z_\phi(t)|^{n-1}z_\varphi(t) - \gamma\tfrac{dx}{d\tau}\dot{\varphi}(t)|z_\varphi(t)|^n, \\ &= \left(A\tfrac{dx}{d\tau} - \beta|\tfrac{dx}{d\tau}||z_\varphi(t)|^{n-1}z_\varphi(t) - \gamma\tfrac{dx}{d\tau}|z_\varphi(t)|^n\right)\dot{\varphi}(t) \\ &= \tfrac{dz}{d\tau}\dot{\varphi}(t), \\ z_\phi(0) &= z_0. \end{aligned}$$

It follows that

$$z_\varphi(t) = z(\varphi(t)),$$

and so

$$\begin{aligned} \Phi_\varphi(t) &= \alpha k x(\varphi(t)) + (1-\alpha)kz(\varphi(t)), \\ &= \Phi(\varphi(t)). \end{aligned}$$

Thus, the Bouc-Wen model (22) describes a rate-independent operator $x \to \Phi$. Since it is clearly causal, it describes a hysteresis operator. Although the Bouc-Wen model is useful for modelling some types of friction, other situations are better described by different models [46–50, e.g.].

8 Conclusions

A number of examples from different contexts that display typical hysteretic behaviour have been discussed in this paper. The examples come from quite different physical applications, but they all display the loops typical of hysteretic behaviour in their input-output graphs. The models discussed here can be put into two groups.

The first group of models are the differential equations used to model the Schmitt trigger, cellular signaling and a beam in a magnetic field. These systems all possess, for a range of constant inputs, several stable equilibrium points. Also, the rate at which the system moves to equilibrium is generally considerably faster than the rate at which the input is changed. Such systems will initially be in one equilibrium, and will tend to stay at that equilibrium point as the input is varied. Varying the input to the point that this equilibrium point disappears causes the system to move to the second equilibrium point. When this move to the new equilibrium happens much faster than the time scale of the system, this change appears instantaneous and the system is only observed in equilibrium. If the system is only observed in equilibrium changes in the input rate do not affect the output and such a system can be said to be rate-independent. If the input rate is increased to become comparable with the system time scale, or if there are other effects on the system, such as thermal dynamics, then rate dependence will be observed.

The second group of models is truly rate-independent. This includes the play operator, the Preisach model for smart materials and the Bouc-Wen model for inelastic springs. These models rely on a equilibrium description of the system and have input-output maps that are independent of the

input rate. The validity of these models in describing the actual physical situation relies on the underlying assumption that the internal dynamics in the system are much faster than the rate at which inputs are varied, and also that other transient effects, such as thermal activation, can be neglected. Since the model is an equilibrium description, any solution of the equations with a constant input is an equilibrium solution. These models possess a continuum of equilibrium points. The assumption that the system is always in equilibrium is a simplification of the dynamics. However, in many situations, this simplication is reasonable and allows for efficient simulations.

This analysis gives a reason for why hysteretic systems can be difficult to control. Controllers for nonlinear systems are often designed using a linearization of the system about an equilibrium point. This approach is useful in applications where the system operates near an equilibrium point. However, under normal conditions, where hysteresis is apparent, hysteretic systems are operated around different equilibrium points. Controllers based on a linearization around a particular operating point will not generally be effective.

It should be clear now that hysteresis is a phenomenon displayed by forced dynamical systems that have several equilibrium points; along with a time scale for the dynamics that is considerably faster than the time scale on which inputs vary. There may be other dynamic effects that lead to a hysteretic system displaying rate dependence under normal operation; see for instance the discussion of smart materials in section 6. However, the essential feature of movement to equilibrium on a time-scale faster than that of the input rate remains. This suggests the following definition.

Definition 3. *A hysteretic system is one which has (1) multiple stable equilibrium points and (2) dynamics that are considerably faster than the time scale at which inputs are varied.*

Thus, hysteresis can be regarded as a property of a dynamical system and its operation, rather than a particular class of systems. An understanding of hysteretic systems can be obtained by an analysis of the multistability displayed by them.

Acknowledgements

The author is grateful to Brian Ingalls and Ralph Smith for useful suggestions on a draft of the manuscript.

References

[1] Brokate, M., and Sprekels, J., 1996. *Hysteresis and phase transitions*. Springer, New York.

[2] Gardner, T. S., Cantor, C. R., and Collins, J. J., 2000. "Construction of a genetic toggle switch in *escherichia coli*". *Nature,* **403**, January, pp. 339–342.

[3] Kennedy, M. P., and Chua, L. O., 1991. "Hysteresis in electronic circuits: A circuit theorist's perspective". *International Journal of Circuit Theory and Applications,* **19**, pp. 471–515.

[4] Mayergoyz, I., 2003. *Mathematical Models of Hysteresis and their Applications*. Elsevier.

[5] Moon, F., and Holmes, P. J., 1979. "A magnetoelastic strange attractor". *Journal of Sound and Vibration,* **65**(2), pp. 275–296.

[6] Smith, R. C., 2005. *Smart material systems: model development*. Frontiers in Applied Mathematics. Society of Industrial and Applied Mathematics, Philadelphia.

[7] Ewing, J. W., 1885. "Experimental researches in magnetism". *Transactions of the Royal Society of London,* **176**, pp. 523–640.

[8] Merriam-Webster, 2012. online dictionary. http://www.merriam-webster.com/.

[9] Brokate, M., 1994. "Hysteresis operators". In *Phase transitions and hysteresis*, A. Visintin, ed. Springer-Verlag, pp. 1–38.

[10] Visintin, A., 1994. *Differential Models of Hysteresis*. Springer-Verlag, New York.

[11] Gorbet, R. B., Wang, D. W. L., and Morris, K. A., 1998. "Preisach model identification of a two-wire SMA actuator". In Proceedings of the IEEE International Conference on Robotics and Automation, Vol. 3, pp. 2161–7.

[12] Logemann, H., Ryan, E. P., and Shvartsman, I., 2007. "Integral control of infinite-dimensional systems in the presence of hysteresis: an input-output approach". *ESAIM - Control, Optimisation and Calculus of Variations,* **13**(3), pp. 458–483.

[13] Logemann, H., Ryan, E. P., and Shvartsman, I., 2008. "A class of differential-delay systems with hysteresis: asymptotic behaviour of solutions". *Nonlinear Analysis,* **69**(1), pp. 363–391.

[14] Ilchmann, A., Logemann, H., and Ryan, E. P., 2010. "Tracking with prescribed transient perfromance for hysteretic systems". *SIAM J. Control and Optimization,* **48**(7), pp. 4731–4752.

[15] Valadkhan, S., Morris, K. A., and Khajepour, A., 2010. "Stability and robust position control of hysteretic systems". *Robust and Nonlinear Control,* **vol. 20**, pp. pg. 460–471.

[16] Oh, J., and Bernstein, D. S., 2005. "Semilinear duhem model for rate-independent and rate-dependent hysteresis". *IEEE Transactions on Automatic Control,* **50**(5), pp. 631–645.

[17] Bertotti, G., 1998. *Hysteresis in Magnetism*. Academic Press.

[18] Macaki, J. W., Nistri, P., and Zecca, P., 1993. "Mathematical models of hysteresis". *SIAM Review,* **35**(1), pp. 94–123.

[19] Schmitt, O. H., 1938. "A thermionic trigger". *Journal of Scientific Instruments,* **15**(1), pp. 24–26.

[20] Harkness, J., 2002. "A lifetime of connections: Otto Herbert Schmitt, 1913-1998". *Physics in Perspective,* **4**, pp. 456–490.

[21] Sedra, A. S., and Smith, K. C., 1982. *Microelectronic Circuits*. Holt Rinehart and Wilson.

[22] Khalil, H. K., 2002. *Nonlinear Control Systems*. Prentice-Hall.

[23] Cherry, J. L., and Adler, F. R., 2000. "How to make a biological switch". *Journal of Theoretical Biology,* **2003**, pp. 117–133.

[24] Angeli, D., and Sontag, E., 2003. "Monotone control systems". *IEEE Transactions on Automatic Control,* **48**(10), pp. 1684–1699.

[25] Angeli, D., and Sontag, E., 2004. "Multi-stability in monotone input/output systems". *Systems and Control Letters,* **51**(3-4), pp. 185–202.

[26] Angeli, D., Ferrell, J. E., and Sontag, E. D., 2004. "Detection of multistability, bifurcations, and hysteresis in a large class of biological positive-feedback systems". *Proceedings of the National Academy of Science,* **101**(7), pp. 1822–1827.

[27] Laurent, M., and Kellershohn, N., 1999. "Multistability: a major means of differentiation and evolution in biological systems". *Trends Biochem. Sci.,* **24**, pp. 418–422.

[28] E.Kurt, 2005. "Nonlinear responses of a magnetoelastic beam in a step-pulsed magnetic field". *Nonlinear Dynamics,* **45**, pp. 171–182.

[29] Guckenheimer, J., and Holmes, P., 1983. *Nonlinear Oscillations, Dynamical Systems, and Bifurcations of Vector Fields*. Springer-Verlag.

[30] Bowong, S., Kakmeni, F. M., and Dimi, J. L., 2006. "Chaos control in the uncertain duffing oscillator". *Journal of Sound and Vibration,* **292**(3-5), pp. 869–880.

[31] Nijmeijer, H., and Berkhuis, H., 1995. "On Lyapunov control of the Duffing equation". *IEEE Transactions on Circuits and Systems,* **42**(8), pp. 473–477.

[32] Valadkhan, S., Morris, K. A., and Khajepour, A., 2009. "A review and comparison of hysteresis models for magnetostrictive materials". *Journal of Intelligent Material Systems and Structures,* **20**(2), pp. 131–142.

[33] Smith, R. C., Dapino, M. J., and Seelecke, S., 2003. "Free energy model for hysteresis in magnetostrictive transducers". *Journal of Applied Physics,* **93**(1), January, pp. 458–466.

[34] Valadkhan, S., Morris, K. A., and Shum, A., 2010. "A new load-dependent hysteresis model for magnetostrictive material". *Smart materials and structures,* **19**(12), pp. 1–10.

[35] Gorbet, R. B., Morris, K. A., and Wang, D. W. L., 1998. "Control of hysteretic systems: a state-space approach". In *Learning, control, and hybrid systems*, Y. Yamamoto, S. Hara, B. A. Francis, and M. Vidyasagar, eds. Springer-Verlag, New York, pp. 432–451.

[36] Achenbach, M., 1989. "A model for an alloy with shape memory". *International Journal of Plasticity,* **5**, pp. 371–395.

[37] Tan, X., and Baras, J., 2004. "Modelling and control of hysteresis in magnetostrictive actuators". *Automatica,* **40**, pp. 1469–1480.

[38] Vainchtein, A., 2002. "Dynamics of non-isothermal martensitic phase transitions and hysteresis". *International Journal of Solids and Structures,* **39**(13-14), pp. 3387–3408.

[39] Ikhouane, F., and Rodeller, J., 2007. *Systems with Hysteresis: Analysis, Identification and Control using the Bouc-Wen model*. Wiley.

[40] Sivaselvan, M. V., and Reinhorn, A. M., 2000. "Hysteretic models for deteriorating inelastic structures". *Journal of Engineering Mechanics,* **126**(6), pp. 633–640.

[41] Gerolymos, N., and Gazetas, G., 2006. "Development of Winkler model for static and dynamic response of caisson foundations with soil and interface nonlinearities". *Soil Dynamics and Earthquake Engineering,* **26**(5), pp. 363–376.

[42] Badoni, D., and Makris, N., 1996. "Nonlinear response of single piles under lateral inertial and seismic loads". *Soil Dynamics and Earthquake Engineering,* **15**, pp. 29–43.

[43] Yi, F., Dyke, S. J., Caicedo, J. M., and Carlson, J., 2001. "Experimental verification of multi-input seismic control strategies for smart dampers". *Journal of Engineering Mechanics,* **127**(11), pp. 1152–1164.

[44] Awrejcewicz, J., and Olejnik, P., 2005. "Analysis of dynamic systems with various friction laws". *Applied Mechanics Reviews,* **58**(6), pp. 389–410.

[45] Bastien, J., Michon, G., Manin, L., and Dufour, R., 2007. "An analysis of the modified Dahl and Masing models: application to a belt tensioner". *Journal of Sound and Vibration,* **302**, pp. 841–864.

[46] Campbell, S. A., Crawford, S., and Morris, K. A., 2008. "Friction and the inverted pendulum stabilization problem". *Journal of Dynamic Systems, Measurement and Control,* **130**(5), pp. 054502–1–054502–7.

[47] Drincic, B., and Bernstein, D. S., 2011. "A Sudden-Release Bristle Model that Exhibits Hysteresis and Stick-Slip Friction". In 2011 American Control Conference, IEEE, pp. 2456–2461. San Francisco, USA.

[48] Freidovich, L., Robertsson, A., Shiriaev, A., and Johansson, R., 2010. "LuGre-model-based friction compensation". *IEEE Transactions on Control Systems Technology,* **18**(1), pp. 194–200.

[49] Márton, L., and Lantos, B., 2009. "Control of mechanical systems with Stribeck friction and backlash". *Systems Control Lett.,* **58**(2), pp. 141–147.

[50] Padthe, A. K., Drincic, B., Oh, J., Rizos, D. D., Fassois, S. D., and Bernstein, D., 2008. "Duhem modeling of friction-induced hysteresis". *Control Systems Magazine,* **28**(5), pp. 90–107.

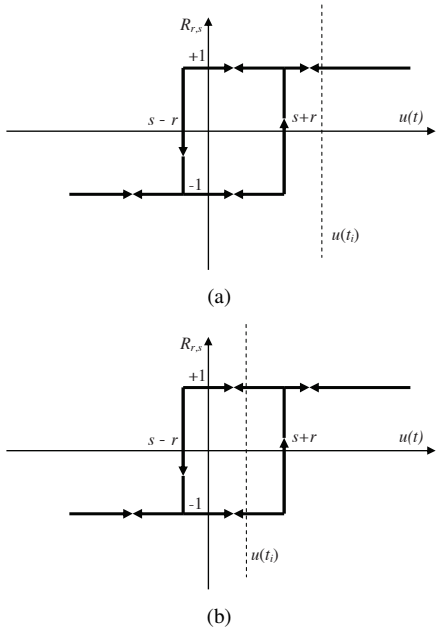

Fig. 1. Simple relay centred on s with width $2r$. The output is unambiguous for $u > s+r$ or $u < s-r$. However, for $s-r < u < s+r$, the output depends on whether the input is increasing or decreasing. (a) $u(t_i) > s+r$, output $+1$ (b) $s-r < u(t_i) < s+r$, output ± 1.

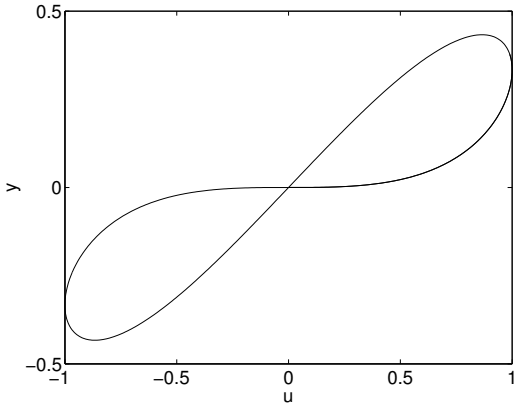

Fig. 3. Loop in the input-output graph of $\ddot{y}(t) + 4y(t) = u(t)$, $u(t) = sin(t), t = 0..8$

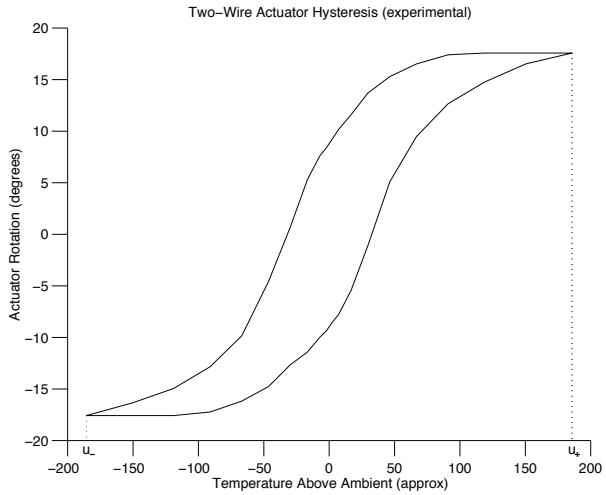

Fig. 2. Temperature-strain curve in a shape memory alloy. The curve depends on the temperature history, but not the rate at which temperature is changed. ©1998, IEEE. Reprinted, with permission, from [11].

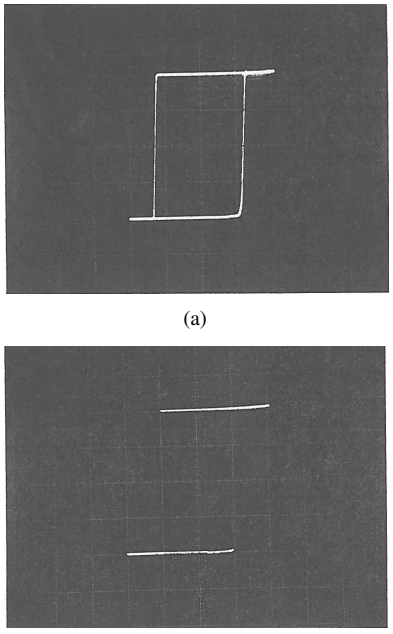

Fig. 4. Experimentally measured voltage for Schmitt trigger. The graphs are similiar to those of a simple relay (Figure 1). (a) input frequency 10 kHz (b) input frequency close to DC. ©1991, Wiley. Reprinted, with permission, from [3].

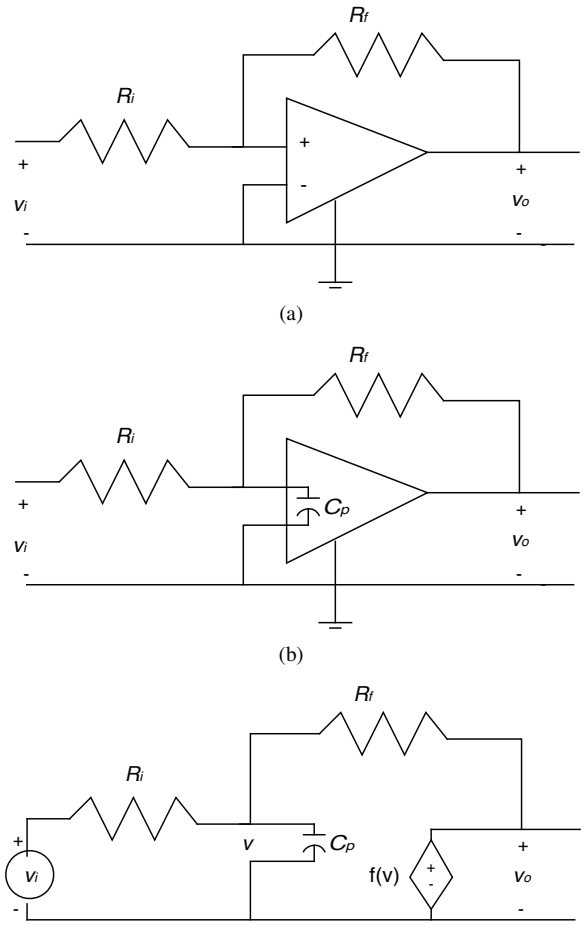

Fig. 5. Schmitt trigger circuit diagrams. (a) standard circuit diagram (b) circuit diagram with input capacitance (c) equivalent circuit to (b) Inclusion of the input capacitance (shown in (b) and (c)) leads to a differential equation model that correctly predicts the response of the circuit. ©1991, Wiley. Used, with permission, from [3].

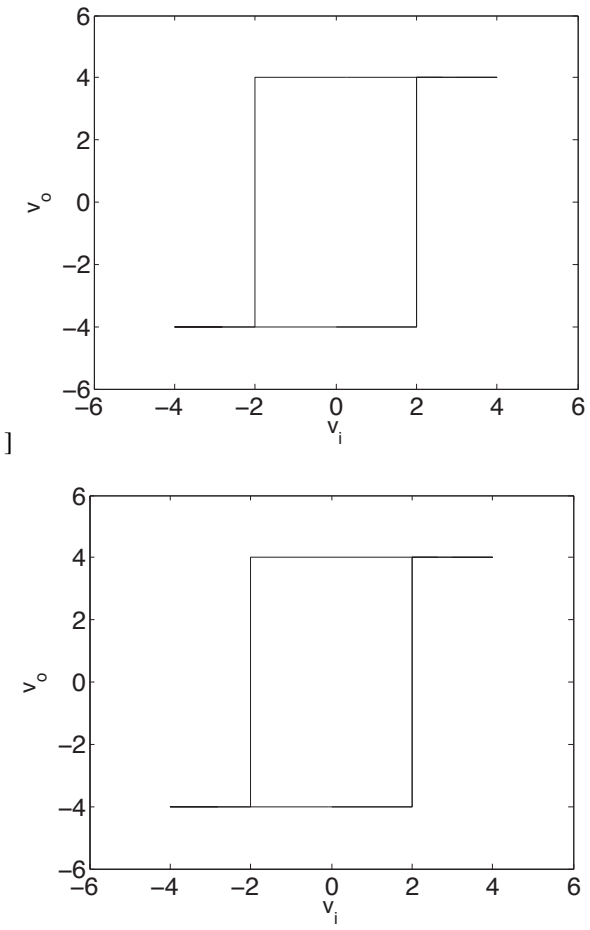

Fig. 6. Simulation of differential equation (3) for Schmitt trigger with the same capacitor initial condition $v(0) = -1$ and different periodic inputs. The response is similar to that of a simple relay and is independent of the frequency of the input. (a) Input $v_i(t) = \sin(t)$ for $7s$ (b) Input $v_i(t) = \sin(10t)$ for $.7s$. (Parameter values $R_i = 10k\Omega$, $R_f = 20k\Omega, A = 10^5, E = 4V, C_p = 15\ pF.$)

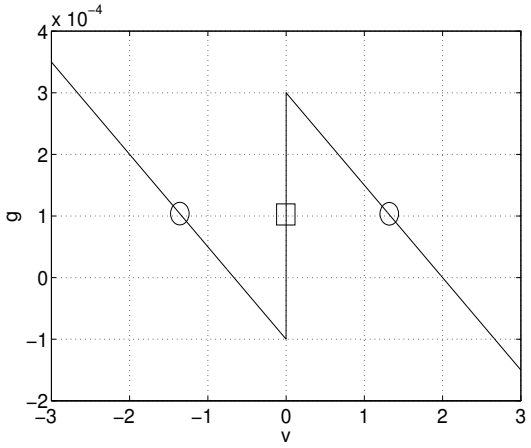

Fig. 7. $g(v_i, v)$ (see (2)) as a function of v with input voltage $v_i = 1$. At this input voltage there are 3 zeros of g and hence the trigger has 3 equilibrium points. The middle zero (□) is an unstable equilibrium while the other two zeros (○) are stable equilibria. For larger values of v_i the graph is higher and for $v_i > 2$ there is only 1 zero of g and hence only 1 equilibrium point. Similarly, for smaller values of v_i the graph is lower and if $v_i < -2$ there is only 1 equilibrium point. (Same parameter values as in Figure 6.)

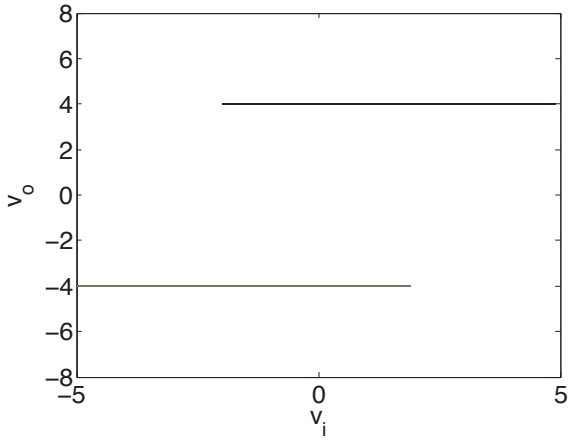

Fig. 8. Output voltage v_o as a function of input voltage v_i for the Schmitt trigger. (See (1, 2).) For $-2 < v_i < 2$ there are 2 possible outputs due to two stable equilibrium values of the capacitor voltage. (Same parameter values as in Figure 6.)

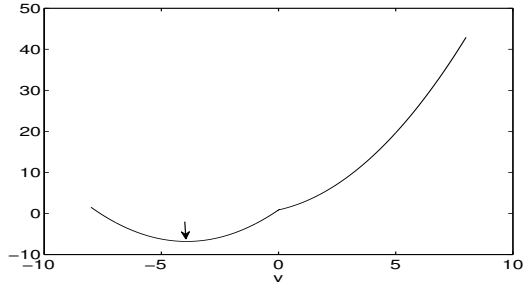

(a)

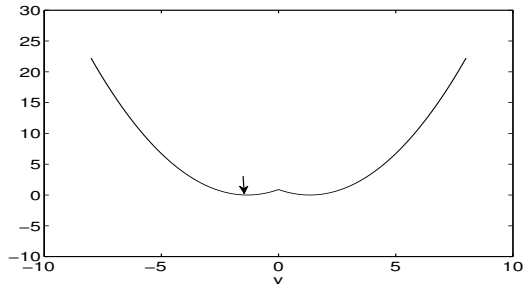

(b)

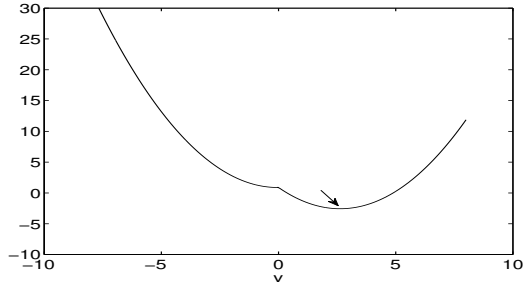

(c)

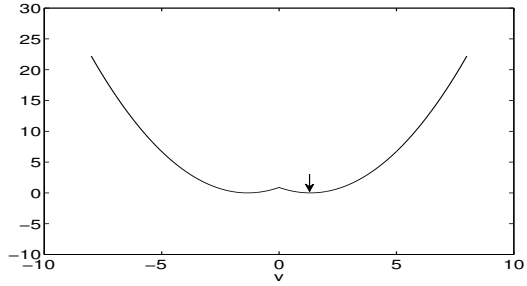

(d)

Fig. 9. Lyapunov function (4) for Schmitt trigger (3) with different input voltages v_i as v_i increases from $-2v_{crit}$ to v_{crit} and then decreases to 0. The arrow indicates the equilibrium capacitor voltage v. It remains at an equilibrium point until v_i changes enough that the Lyapunov function no longer has a minimum at that point. (a) Input voltage $v_i = -2v_{crit}$. There is one equilibrium voltage. (b) Input voltage increases to $v_i = 0$. There are now 2 minima; v remains at the left-hand minimum. (c) Input voltage increases to $v_i = v_{crit}$. The left-hand minimum disappears; v moves to the only minimum. (d) Input voltage decreases to $v_i = 0$. There are again two minima of the Lyapunov function; v remains at the current minimum. (Same parameter values as in Figure 6.)

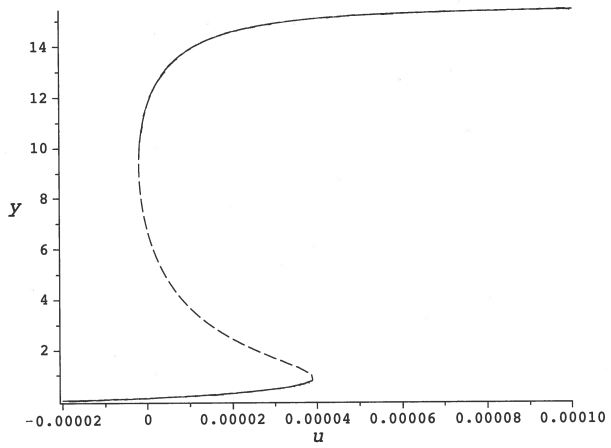

Fig. 10. Equilibrium value of output y (concentration of protein x_2) at different values of the input IPTG (u). There are 3 equilibrium values if $-10^{-6} < u < 4 \times 10^{-5}$. The middle one is unstable, while the other two equilibria are stable. (See (5,6,7). Parameter values of $\alpha_1 = 156.25, \beta_1 = 2.5, \alpha_2 = 15.6, \beta_2 = 1, K = 2.9618 \times 10^{-5}$ and $\eta = 2.0015$ from [2] .)

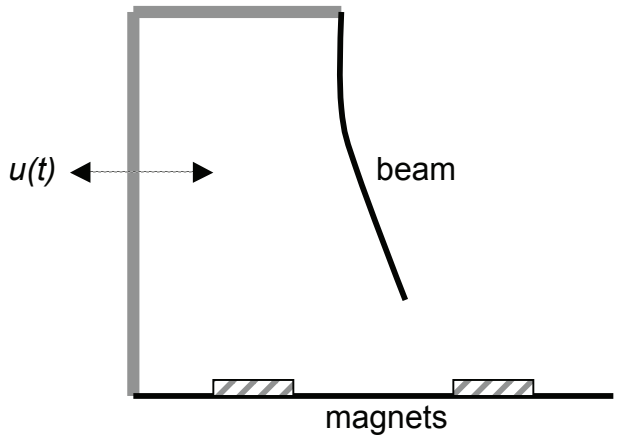

Fig. 12. Beam in a magnetic field with two magnetic sources

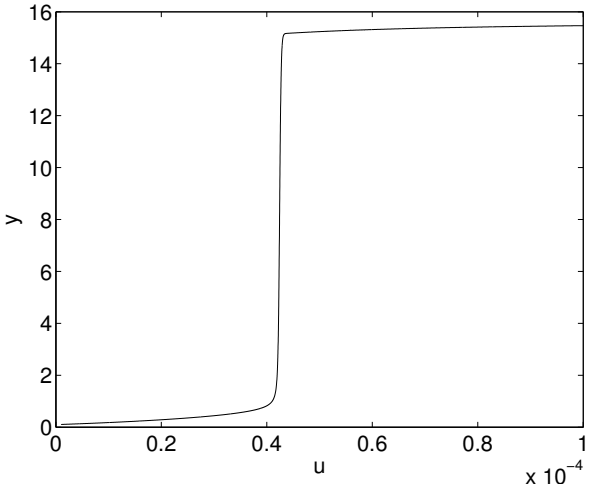

Fig. 11. Output y (concentration of x_2) as u is slowly increased. Note sharp transition to new equilibrium point. (See (5,6,7). Same parameter values as in Figure 10.)

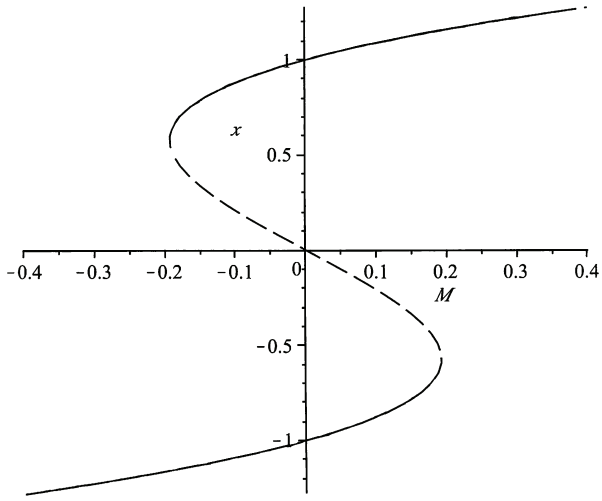

Fig. 13. The equilibrium points of beam (9) in a two-source magnetic field M are the roots of $\frac{1}{2}x(1-x^2) + M = 0$. For $|M| < \frac{1}{3\sqrt{3}} \approx 0.2$ there are 3 solutions of $f(x) = M$ while for larger values of M there is only one solution. Hence for small amplitudes of the magnetization there are 3 equilibrium points while for larger amplitudes there is only 1 equilibrium point. When there are 3 equilibrium points, the middle point is unstable while the outer points are stable.

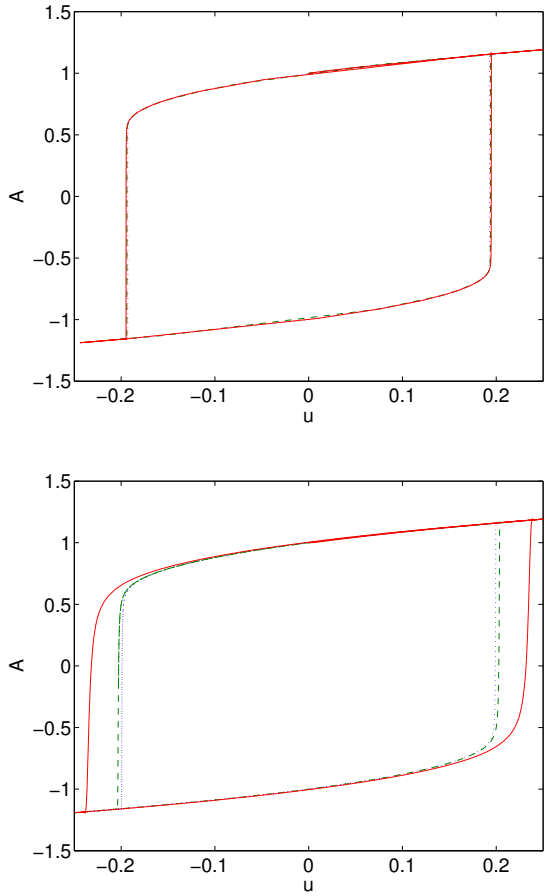

Fig. 14. Input-output diagram for magneto-elastic beam (9) with input $\frac{1}{4}\sin(\omega\tau)$, with different frequencies ω. Looping behaviour as the state moves between different equilibrium points is evident. (a) $\omega = 10^{-5}\,(\cdots), 5\times10^{-5}\,(--), 10^{-4}\,(-)$. The three curves are indistinguishable, indicating that the system is rate-independent at low frequencies of the input. (b) $\omega = 5\times10^{-4}\,(\cdots)$, $10^{-3}\,(--)$, $10^{-2}\,(-)$. At these higher frequencies, rate dependence is apparent.

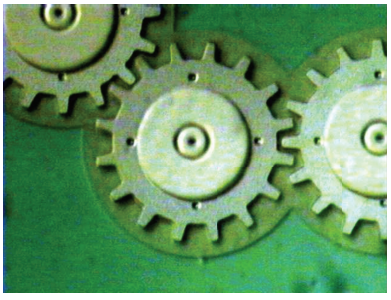

Fig. 15. Gears, showing mechanical play (http://www.sfu.ca/adm/gear.html, used by permission, Robert Johnstone, SFU). Since the gears are not perfectly meshed, when one gear turns there is a period of time when the driven gear is stationary before it engages and is turned by the first gear.

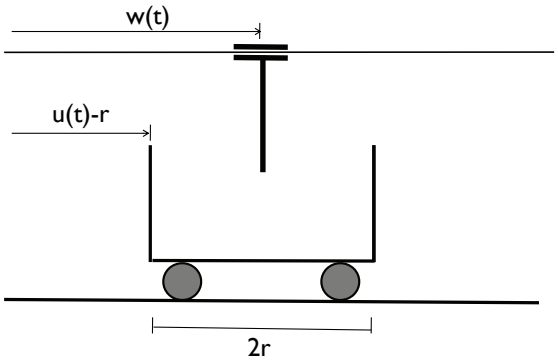

Fig. 16. Backlash, or linear play. The rod with position $w(t)$ is moved by a cart of width $2r$ with centre position $u(t)$. As long as the rod remains within the interior of the cart, the rod does not move. Once one end of the cart reaches the rod, the rod will move with the cart.

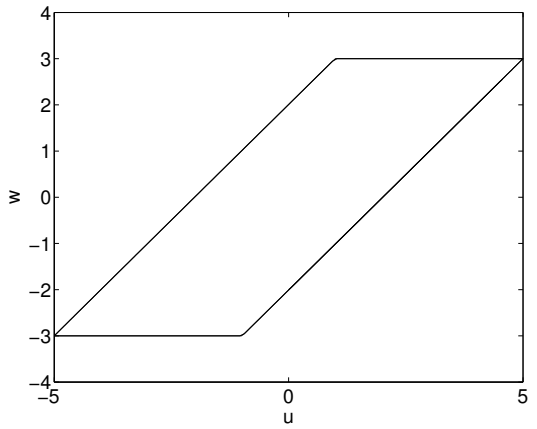

(a)

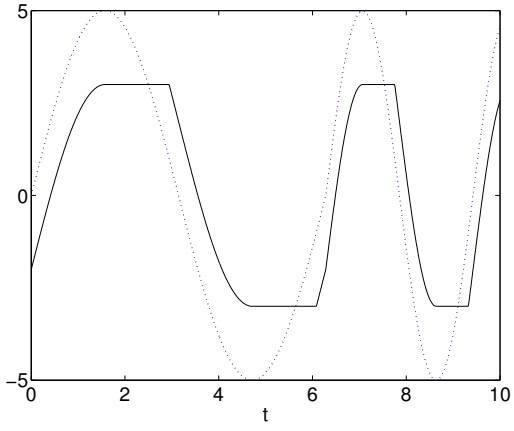

(b)

Fig. 17. Play operator with play $r = 2$. (a) input-output diagram, static model (12) and dynamic model (13). ($a = 1000$ for dynamic model) The graphs of the dynamic and static models are indistinguishable. (b) input u $(\cdots)$ and output w $(-)$ Note that w remains constant after a change in sign of $\dot{u}$ until the difference $|w-u| = 2$.

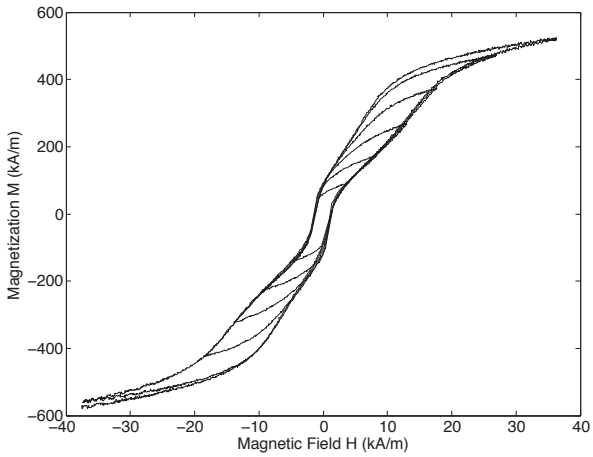

Fig. 18. Magnetization versus magnetic field for a magnetostrictive actuator [32, used with permission]. The outer, or major, loop is obtained by increasing the input magnetic field to its maximum value and then subsequently decreasing it. The inner loops are obtained by increasing the input to an intermediate value and then decreasing.

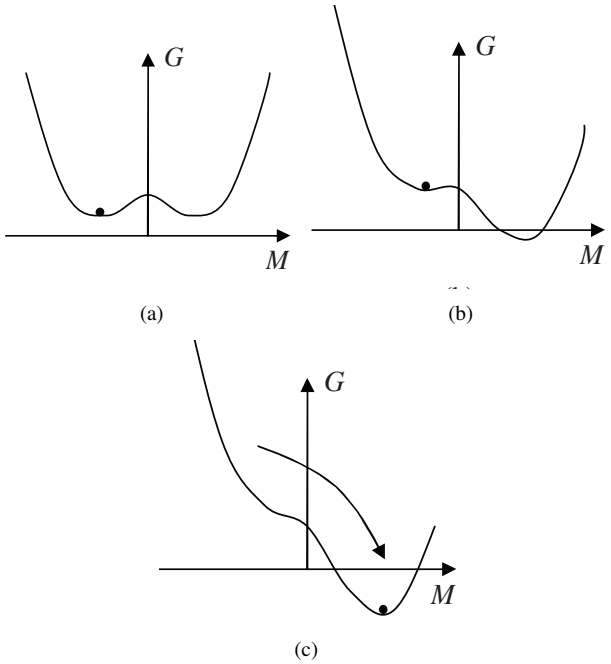

Fig. 19. Qualitative behaviour of Gibb's energy for a magnetic dipole as H is varied. (a) Gibbs energy when $H_0 = 0$. There are two equilibrium points, M_-^* and M_+^*. In this diagram, the dipole is at M_-^*. (b) Gibbs energy after increasing H_0 where there are still two equilibrium points. The dipole remains at M_-^*. (c) If H_0 is further increased, eventually only one minimum exists. The dipole moves to the remaining minimum, M_+^*.

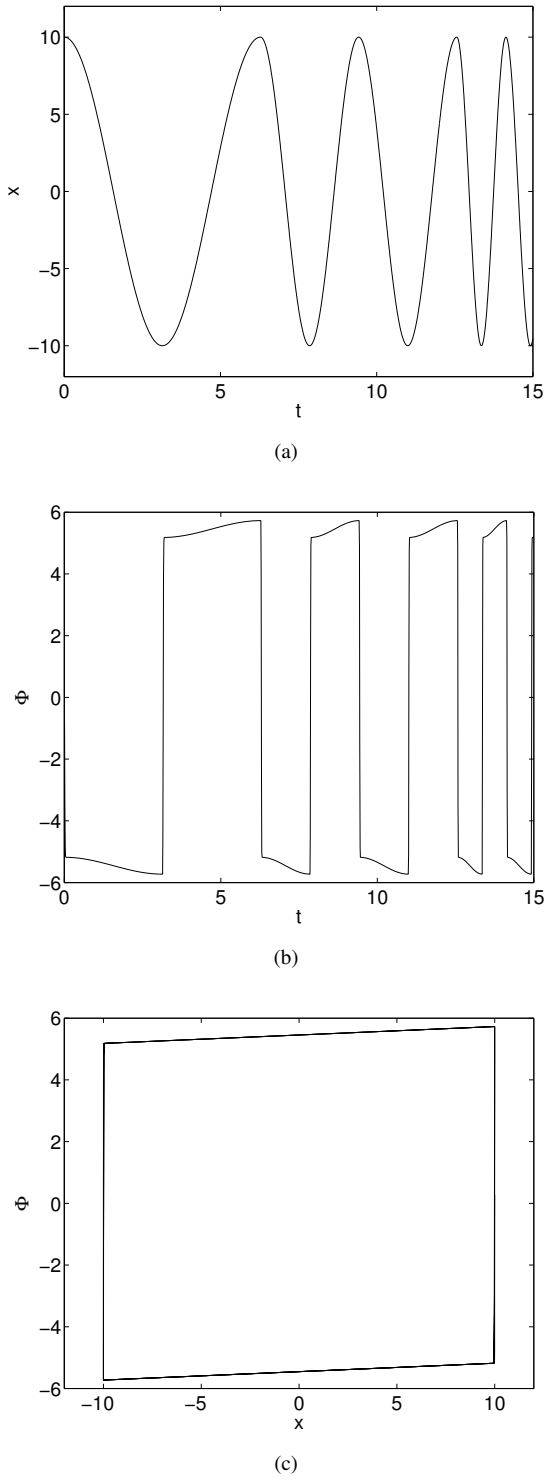

Fig. 20. Response of Bouc-Wen model (22). (a) Input $x(t)$ with varying frequency (b) output $\Phi(t)$ for input shown in (a) . Only the scale, not the shape of the curve, changes as the input frequency changes. (c) $\Phi(t)$ versus input $x(t)$ shown in (a) . The curve forms a single loop, reflecting rate independence of the model. (Parameter values are those used in identification of a magnetorheological damper in [43]: $D = 1$, $n = 1$, $A = 120$, $\gamma = 300cm^{-3}$, $\beta = 300cm^{-1}$, $\alpha = 0.001$, $k = 27.3Ns/cm$.)

List of Figures